water

MDPI

Article

Electrochemical Oxidation of Reverse Osmosis Concentrates from Landfill Leachate Treatment Using Ti_4O_7-Nanotube Reactive Electrochemical Membrane

Qiujie Qian, Pingzhong Xiao, Tinghui Du, Demin Xu, Chuanshuo Guo, Yue Guan, Minxuan Yan, Feihong Wang, Yonghao Zhang * and Yan Li *

School of Environmental Science and Engineering, Yancheng Institute of Technology, Yancheng 224051, China; qianqj_ycit@163.com (Q.Q.); xiaopz041108@163.com (P.X.)
* Correspondence: zyhlygxp@163.com (Y.Z.); leeyeon0610@163.com (Y.L.)

Abstract: With the growing demand for high-quality discharge, reverse osmosis (RO) technology has been widely applied in landfill leachate treatment; however, the problem of reverse osmosis concentrates (ROCs) has worsened. In this work, a Ti_4O_7-nanotube reactive electrochemical membrane (Ti_4O_7-NT-REM) was employed to treat ROCs from landfill leachate treatment. The effects of current density, flow rate and pH on COD removal were evaluated, and the appropriate conditions were a current density of 20 mA cm^{-2}, a flow rate of 10 mL s^{-1} and a pH of 7. Under these conditions, COD, TOC, NH_4^+-N and NO_3^--N were removed by 82%, 68%, 100% and 73%, respectively. In addition, the 3D-EEM fluorescence spectra and GC–MS results revealed that the organics significantly decreased after 120 min of treatment, and aliphatic compounds were the major organic compounds. The stable performance of the REM was illustrated by cyclic treatment (20 cycles) with the assistance of cathodic polarization. In addition, a long service lifetime of 267.3 h and a low energy consumption of 7.6 kWh·kg COD^{-1} were obtained by related testing and evaluation. The excellent and stable performance confirmed that the Ti_4O_7-NT-REM has broad application prospects in the treatment of ROCs.

Keywords: electrochemical oxidation; actual reverse osmosis concentrates; Ti_4O_7-nanotube reactive electrochemical membrane (Ti_4O_7-NT-REM); long service lifetime; energy efficient

Citation: Qian, Q.; Xiao, P.; Du, T.; Xu, D.; Guo, C.; Guan, Y.; Yan, M.; Wang, F.; Zhang, Y.; Li, Y. Electrochemical Oxidation of Reverse Osmosis Concentrates from Landfill Leachate Treatment Using Ti_4O_7-Nanotube Reactive Electrochemical Membrane. *Water* **2024**, *16*, 3579. https://doi.org/10.3390/w16243579

Academic Editor: Christos S. Akratos

Received: 13 November 2024
Revised: 7 December 2024
Accepted: 9 December 2024
Published: 12 December 2024

1. Introduction

Water shortages have long been an important factor restricting the development of human society, and China is designated a water-deficient country with low water resources per capita [1,2]. Wastewater recycling is a promising strategy and necessary approach to address this critical problem. For many recycling strategies, reverse osmosis (RO) technology emerged as a promising method in wastewater treatment, one of which is landfill leachate treatment [3–5]. However, the RO system achieves high-quality effluents but also produces reverse osmosis concentrates (ROCs) at percentages between 30% and 40% of the incoming wastewater [6]. This generated ROC usually involves increased salinity and high concentrations of inorganic ions and refractory organic pollutants [7,8]. Moreover, some chemicals (e.g., disinfectants, reducing agents and anti-scaling agents) that maintain RO system performance often unavoidably exist in ROCs [9]. With the continuous expansion of the scope and quantity of the RO process in landfill leachate treatment worldwide, the amount of ROC is also increasing. Direct discharge of this type of wastewater severely threatens the water environment. Therefore, there is an urgent need to find an effective method to address ROCs before discharge. Recently, various methods, including evaporation, coagulation, adsorption, biological treatment and advanced oxidation processes (AOPs), have been investigated to treat ROC, aiming to remove refractory organics and reduce biological toxicity [10].

To address the refractory and toxic organic pollutants of ROC, AOPs are considered effective because they can generate strong oxidants of OH· either by photocatalysis, electrocatalysis or reactions between chemicals, such as ultraviolet oxidation, electrochemical oxidation (EO), Fenton oxidation or ozone-based oxidation [11–14]. Among them, EO is more suitable for ROC treatment because it adapts to high-salinity circumstances and also can take advantage of salt to generate various new oxidants, such as reactive chlorine species (RCS) and sulfate radicals [5,15]. Currently, EO is extensively used in the treatment of ROC, which can not only remove refractory pollutants but also contribute to the removal of conventional indexes, such as COD, BOD_5, ammonium nitrogen (NH_4^+-N) and total nitrogen (TN). However, the traditional EO process involving plate electrodes suffered from poor mass transfer, which results in high energy consumption. To solve this critical problem, reactive electrochemical membranes (REMs) have been developed and subsequently intensively studied in recent years [16–18]. The REMs have been tested in "flow-through" mode instead of "flow-by" mode, which significantly improves the mass transfer efficiency via the convection flow of the solution toward the electrode. Accordingly, REMs have shown great potential in the treatment of ROC.

In addition to the operation mode, the catalytic coating of REMs also plays an important role in EO, and different materials exhibit large differences when removing pollutants. Related studies have reported various catalytic coatings in ROC treatment, including IrO_2, RuO_2-IrO_2, Pd, SnO_2-Sb, PbO_2 and BDD, and some of them referred to REMs [12,19–24]. Among these coatings, nonactive electrodes (e.g., SnO_2, PbO_2, BDD and Ti_4O_7) have a stronger ability to destroy organic pollutants because they weakly interact with the generated OH· [25]. Nevertheless, the SnO_2 electrode suffers from low stability and service life, the PbO_2 electrode faces the challenge of leaching toxic Pb^{2+} and the BDD electrode has a high material and fabrication cost [26,27]. In contrast, Ti_4O_7 has shown great potential in terms of applications because of its great electroconductibility, chemical resistance and relatively low price [28,29]. These properties indicate that Ti_4O_7 is a suitable material for REMs in ROC treatment. In a previous study, we fabricated a Ti_4O_7-nanotube REM (Ti_4O_7-NT-REM), which showed excellent performance in the treatment of ceftriaxone sodium-containing antibiotic wastewater [30]. After treatment, the biodegradability and toxicity of the wastewater significantly increased and decreased, respectively. However, ROCs are more complex in terms of organics and high salinity than the above-mentioned antibiotic wastewater. The performance, durability and cost of Ti_4O_7-NT-REM for the treatment of actual ROC are still unclear. Thus, it is necessary to study the treatment of actual ROCs by Ti_4O_7-NT-REM before large-scale application.

In this study, Ti_4O_7-NT-REM was employed to treat actual ROCs from landfill leachate treatment. The effects of the operation parameters (current density, flow rate and pH) on COD removal were investigated. The performance of REM on the removal of total organic carbon (TOC), NH_4^+-N and NO_3^--N was also investigated. Furthermore, variations in dissolved organic matter (DOM) were studied in detail via 3D-EEM fluorescence spectroscopy and GC–MS. Finally, the long-term stability and operation cost were also investigated.

2. Materials and Methods

2.1. Reactant and Material

The chemicals were analytical grade or higher. Sodium chloride, sulfuric acid, sodium hydroxide, hydrofluoric acid and potassium fluoride dihydrate were purchased from Sigma-Aldrich (Shanghai, China). Dichloromethane for GC–MS was chromatographic grade and obtained from Aladdin Industrial Co., Ltd. (Shanghai, China). The porous Ti substrate was bought from Baoji Yinggao Metal Materials Co., Ltd. (Baoji, China). Ultrapure water was obtained from a Milli-Q® EQ 7000 system (Merck Chemical Technology Co., Ltd., Shanghai, China). The reverse osmosis concentrate sample was obtained by a landfill leachate treatment plant located in Yancheng, China. The RO system was placed after two-stage AO and MBR. The detailed characteristics are shown in Table S1.

2.2. Fabrication of Ti_4O_7-NT-REM

The Ti_4O_7-NT-REM employed in this study was fabricated through our previous study [31]. Briefly, a porous titanium substrate (diameter of 30 mm, thickness of 1 mm, pore size of ~20 μm) was first anodically oxidized in a solution consisting of hydrofluoric acid and potassium fluoride dihydrate to generate TiO_2-NT and then reduced TiO_2-NT into Ti_4O_7-NT by hydrogen at a high temperature to obtain the Ti_4O_7-NT-REM.

2.3. Electrolysis Process

The ROC was electrochemically treated in a reactor assembled with Ti_4O_7-NT-REM, nickel foam and an O-ring (Figure 1). During the process, the reactor was immersed in a container containing 500 mL of ROC. The current was inputted and controlled by a DC power supply (Hanshengpuyuan, Beijing, China). Herein, Ti_4O_7-NT-REM was used as the anode, and nickel foam was used as the cathode. The electrodes were isolated by an O-ring with a distance of 1 cm. During the treatment, the ROC was continually circulated between the reactor and beaker via a peristaltic pump (Longer, Baoding, China), which also can control flow rate. The pH value was adjusted with 1 M H_2SO_4 and NaOH. For cyclic experiments, cathodic polarization was undertaken before each cycle at a current density of 2.5 mA cm^{-2} for 10 min to ensure that the performance achieved was in line with previous methods [32]. Cathodic polarization was achieved by simply reversing the anode and cathode.

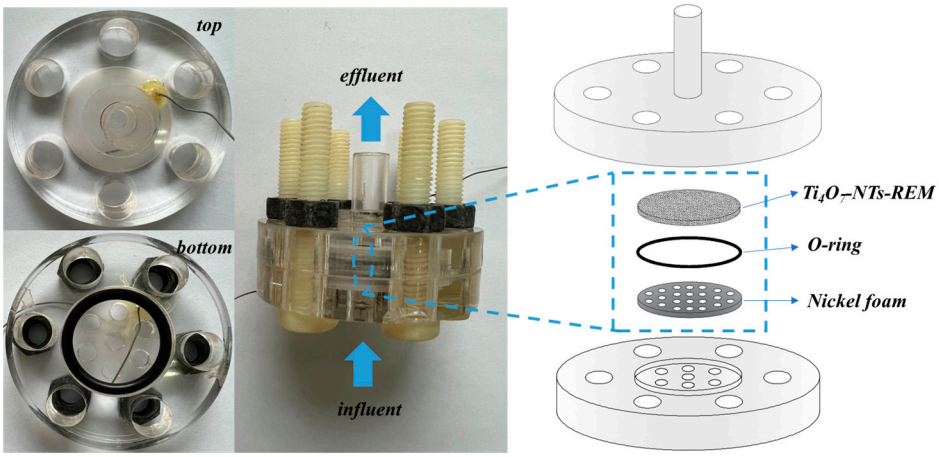

Figure 1. Schematic diagram of Ti_4O_7-NT-REM reactor for the experiments.

2.4. Analytical Methods

The concentrations of COD, NH_4^+-N, NO_3^- and NO_2^- were measured via an LH-5B-3B multiparameter water quality analyzer (Lianhua, Beijing, China) with the corresponding reagents purchased from Beijing Lianhua Co., Ltd. TOC was measured via a TOC analyzer (TOC-LCP H, Shimadzu, Japan). The pH value was measured with a pH meter (PHS-3B, Shanghai Precision & Scientific Instrument Co. Ltd., Shanghai, China). The excitation–emission matrix fluorescence spectroscopy analysis was performed with a spectrophotometer (Horiba, Japan), and the excitation and emission slits were set to 3 nm. The organic composition of ROC was detected via gas chromatographic mass spectrometry (TRACE ISQ, Thermo, Waltham, MA, USA) after extraction with CH_2Cl_2 via a previously reported method (Text S1). The acute toxicity tests were conducted with five *D. magna* neonates (less than 24 h old) in 50 mL test solution at five test concentration gradients with four replicates [33]. Accelerated service life tests were performed at current densities up to 1 A cm^{-2} in ROC and 0.5 M NaCl, respectively. The calculations of removal and energy consumption are presented in Text S2.

3. Results

3.1. ROC Treatment by Ti_4O_7-NT-REM

3.1.1. Contaminant Removal

The removal of COD, TOC, NH_4^+-N and NO_3^--N by Ti_4O_7-NT-REM was evaluated, as shown in Figure 2. Figure 2a–c present the effects of the current density, flow rate and pH on COD removal. The current density is a crucial factor in EO because the degree of molecular transformation and the reaction rate are highly related to the current density [34]. It can be found in Figure 2a that the COD removal increased with increasing current density. The COD concentration was reduced to 82 mg L^{-1} after treatment when the current density was 20 mA cm^{-2}, whereas it was 307, 234 and 102 mg L^{-1} for 5, 10 and 15 mA cm^{-2}, respectively. The higher current density contributes to a high yield of reactive chlorine species (RCS) and ·OH, leading to this high performance. Nevertheless, the improvement in COD removal was not significant (20%) when the current density increased from 15 to 20 mA cm^{-2}. This is attributed to the serious side reactions of O_2 evolution induced by the high current density. Moreover, a high current density also caused the conversion of some electric energy into thermal energy, which resulted in invalid consumption of the given charge [35]. Figure 2b shows the COD removal under different flow rates. Like the current density, the flow rate also has a positive influence on COD removal. This is because of the increased mass transfer from the increasing flow rate. As expected, the COD removal increased when the flow rate increased [36]. The COD concentrations after 12 min of treatment for 4, 6, 8 and 10 mL s^{-1} were 173, 125, 95 and 82 mg L^{-1}, respectively. Furthermore, the improvement in COD removal was almost negligible when the flow rate increased from 8 to mL s^{-1}, indicating that improving the flow rate was inefficient up to 8 mL s^{-1}. To evaluate the effect of pH, the ROC was adjusted to pH 3, 5 and 9 before starting the treatment. Figure 2c shows that acidic conditions are favorable for removing COD. The COD concentration decreased to 42 and 44 mg L^{-1} under acidic conditions (pH 3 and 5), which was lower than that under neutral and alkaline conditions (82 mg L^{-1} for pH 7 and 184 mg L^{-1} for pH 9). This can be explained by the fact that the side oxygen evolution reaction can be alleviated because of the higher oxygen evolution potential in acidic solutions [37]. Moreover, bicarbonate ions (HCO_3^-), which can quench radicals, are eliminated when the pH value was 3 [38]. As presented above, although the conditions of 20 mA cm^{-2} and 10 mL s^{-1} can remove more COD in each comparison, the improvement was not significant when compared with the nearby conditions. Considering that a higher current density and higher flow rate cause considerable electric energy wasting in terms of electrolytic heating and driving forces, the appropriate current density and flow rate for ROC treatment should be 15 mA cm^{-2} and 8 mL s^{-1}, respectively. On the other hand, the COD was efficiently removed at pH 7, and adjusting the pH requires many chemicals (H_2SO_4), which is not economical or environmentally friendly. Thus, no pH adjustment was conducted in later experiments.

In addition, the removal performance of Ti_4O_7-NT-REM for TOC, NH_4^+-N and NO_3^-N was further evaluated. As shown in Figure 2d, 68% of the total organic carbon (TOC) was removed after treatment, indicating that the REM is more suitable for degrading persistent organic matter. Furthermore, NH_4^+-N removal reached approximately 100% after treatment. This is attributed to the generated RCS, which has a high reaction rate with NH_4^+-N. The high removal of NO_3^--N (73%) might be due to cathode reduction by nickel foam, which can generate massive amounts of atomic H* when serving as a cathode [39].

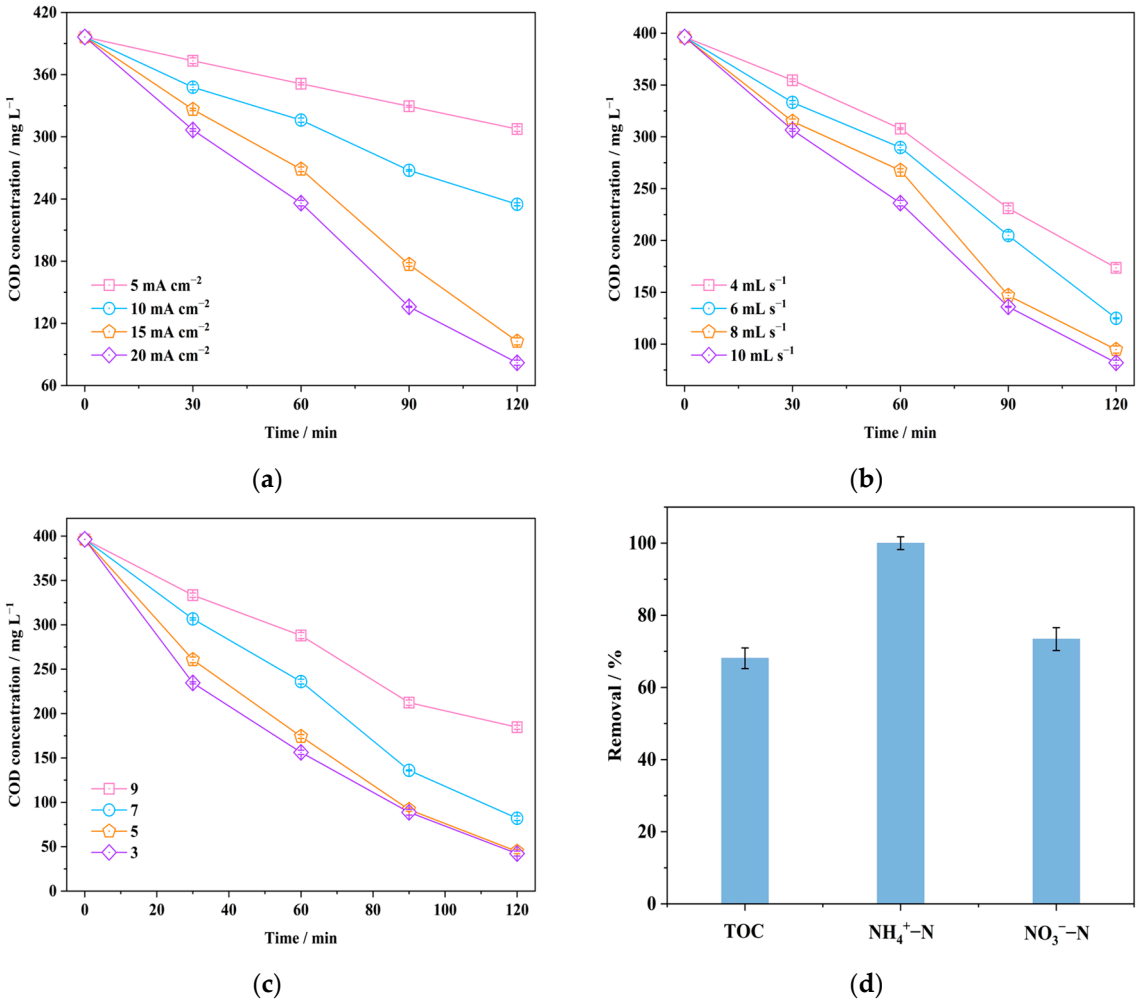

Figure 2. (**a**) The effect of current density on COD removal (conditions: flow rate 10 mL s^{-1}, pH 7); (**b**) the effect of flow rate (conditions: current density 20 mA cm^{-2}, pH 7) on COD removal; (**c**) the effect of pH (conditions: current density mA cm^{-2}, flow rate 10 mL s^{-1}) on COD removal; (**d**) TOC NH_4^+-N and NO_3^--removal for treatment process (conditions: flow rate 8 mL s^{-1}, pH 7 and current density at 15 mA cm^{-2}).

3.1.2. Variations in Dissolved Organic Matter

To evaluate the variation in dissolved organic matter (DOM), Figure 3 presents the 3D-EEM fluorescence spectra obtained during the treatment. According to previous studies, the spectra can be categorized into four regions: aromatic protein substances (I), fulvic acid-like substances (II), soluble microbial byproduct-like substances (III) and HA-like substances (IV) [40]. Apparently, soluble microbial byproduct-like substances and HA-like substances were the predominant components of DOM in ROC, as the majority of the fluorescence intensity is located in regions (III) and (IV). As we can see in Figure 3b, the fluorescence intensity area significantly decreased, and fulvic acid-like and HA-like substances almost disappeared, whereas only a few soluble microbial byproduct-like substances remained. This result illustrated that the strong degradability of Ti_4O_7-NT-REM decomposed HA-like substances into other soluble microbial byproducts after 60 min treatment [41]. Moreover, the fluorescence intensity area was almost completely eliminated from the spectra after 120 min of treatment, as shown in Figure 3c. Only some areas of scattered fluorescence intensity could be found in region (I), indicating that the organics either were mineralized into CO_2 and H_2O or transformed into smaller and non-fluorescent organics.

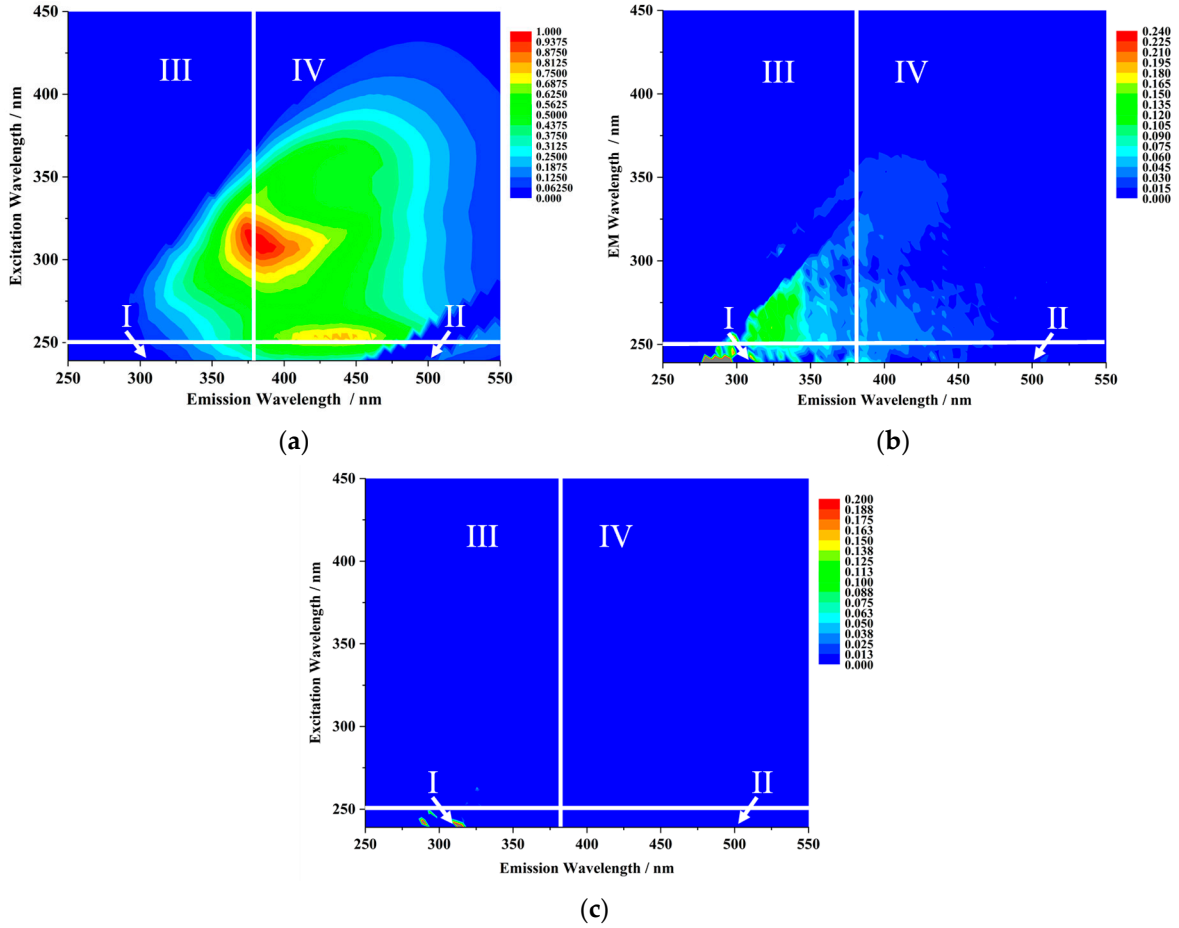

Figure 3. Excitation–emission matrix (EEM) fluorescence spectra of ROC (conditions: flow rate 8 mL s^{-1}, pH 7 and current density at 15 mA cm^{-2}): (**a**) untreated, (**b**) after 60 min treatment and (**c**) after 120 min treatment.

Considering that some DOM (e.g., aliphatic compounds) cannot be reflected directly via 3D-EEM fluorescence spectra, GC–MS was further employed to study the changes in organics. The types and proportions of DOM as well as its sequential degradation are presented in Tables S2 and S3 and Figure S1. As we can see, 43 organics were detected in the influent, while 55 organics were detected in the effluent, which can be classified as aliphatic compounds, aromatic compounds, alcohol compounds, esters, amides, silanes, phenols, ketones, etc. Interestingly, silanes, ketones and alcohols were removed from the ROC after 120 min of treatment, whereas chlorinated compounds were newly detected (Figure 4a). This phenomenon can be attributed to the anticipation of RCSs during treatment, which were generated by the chlorine evolution reaction at the surface of Ti_4O_7-NT-REM (Figure S2) [42]. Figure 4b shows that the range of molecular weight (M.W.) of the organics in the influent was 170~592 g mol^{-1}, and most of the organics had M.W. values of 206, 212, 256, 276, 282, 296 and 478 g mol^{-1}. After 120 min of treatment, the molecular weights of the organics in the effluent were in the range of 124~500 g mol^{-1}, and most organics had M.W. values of 124, 140, 152, 216, 256 and 284 g mol^{-1}. In particular, the organics with M.W. values of 124, 134, 140 and 152 corresponded to the newly generated chlorinated compounds (red circles). In addition, the change in the number of carbon atoms was also investigated (Figure 4c). Figure 4c shows the number of carbon atoms distributed at C10~C39 for the influent and C4~C40 for the effluent. Two significant changes can be observed after treatment: (i) the number of organics with C14~C23 carbon atoms significantly decreased, and (ii) several organics with less carbon atoms (C4~C6) were detected. Combined with the results of the evaluation of M.W. and carbon atoms, these findings indicate that the macromolecular

organics in ROCs were efficiently degraded into smaller molecules through electrochemical treatment. In addition, acute toxicity tests further support the results of the GC–MS study as the IC_{50} values increased from 31.7% to 67.3% (Figure 4d) after treatment, indicating a reduced threat of the treated ROC to the environment.

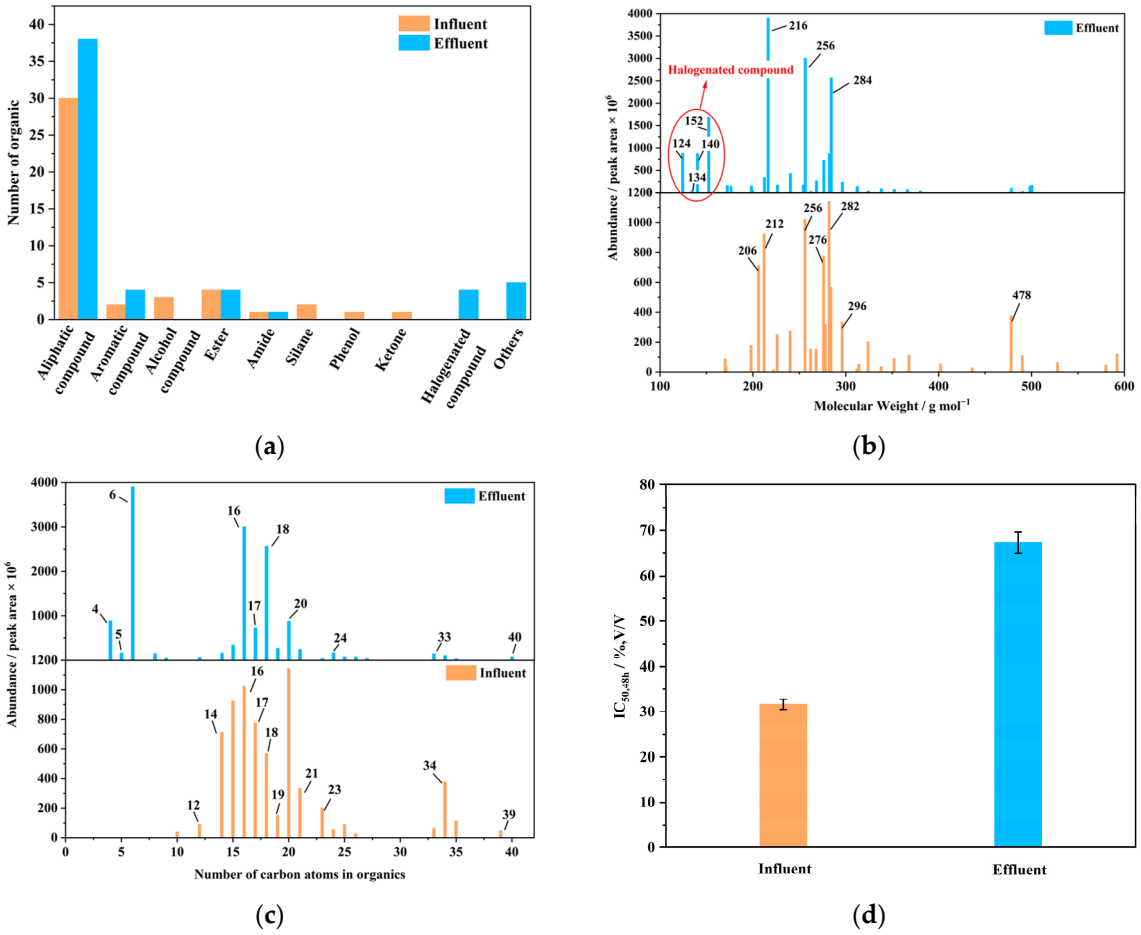

Figure 4. (**a**) Amounts of different organics in influent and effluent; (**b**) distribution of organics with different molecular weight (M.W.) values in influent and effluent; (**c**) carbon atom of organics in influent and effluent and (**d**) IC_{50} value of influent and effluent (conditions: flow rate 8 mL s^{-1}, pH 7 and current density at 15 mA cm^{-2}).

3.1.3. Long-Term Durability

The long-term durability of Ti_4O_7-NT-REM in the ROC treatment was evaluated via cyclic experiments (20 cycles). As shown in Figure 5a, the COD removal rate was maintained within 70~81% over 20 cycles, and the removal rate of the last cycle was 92.7% of that of the first cycle, suggesting the great stability of degrading organics. Figure 5b shows that the REM is highly stable for TOC removal. The fluctuation range of TOC removal was within 13%, and at least 64% of the total organic carbon (TOC) was removed. The removal percentage of the last circle was 90.8% of that of the first circle. For NH_4^+-N (Figure 5c), the REM not only shows stable removal but also exhibits great efficiency. The NH_4^+-N was barely detected in the effluent of any of the circles. Furthermore, the REM still steadily removed NO_3^--N, as shown in Figure 5d. The largest difference in removal was 7%, and the removal decreased by only 4% between the last cycle and the first cycle. In conclusion, 70~81%, 64~78%, 99.1~100% and 68~75% of the COD, TOC, NH_4^+-N and NO_3^--N, respectively, were removed during the cyclic experiments, confirming the high long-term durability of the Ti_4O_7-NT-REM. Moreover, the mean concentrations of COD, TOC, NH_4^+-N and NO_3^--N in the effluent were 93, 29, 0.10 and 8.1 mg L^{-1}, respectively.

The treated ROC met the standard for pollution control at the landfill site of municipal solid waste in China (GB16889-2008) (Table S1) [43], indicating that the ROC can now be discharged. In addition, Figure S3 displays the SEM images of Ti_4O_7-NT-REM before and after 20 cycles, where the REM still possesses a compact nano-structure after long-term study and even some cracking and impurities could be observed. These results strongly support the durability of Ti_4O_7-NT-REM.

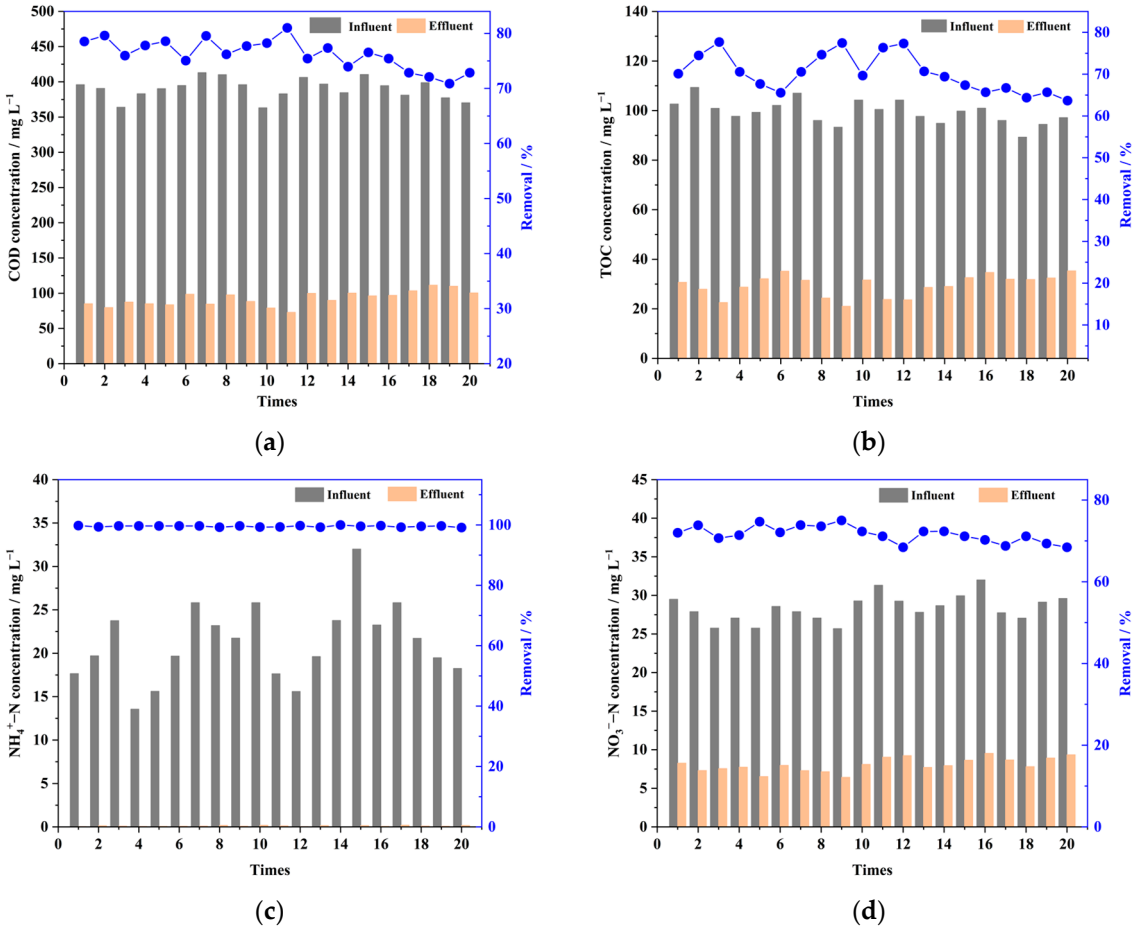

Figure 5. (**a**) The COD concentration of the influent and effluent over 20 cycles; (**b**) the TOC concentration of the influent and effluent over 20 cycles; (**c**) the NH_4^+-N concentration of the influent and effluent over 20 cycles; (**d**) the NO_3^--N concentration of the influent and effluent over 20 cycles (conditions: flow rate 8 mL s^{-1}, pH 7 and current density at 15 mA cm^{-2}).

3.1.4. Service Lifetime and Energy Consumption Evaluation

The service lifetime of REMs is a core factor for actual application. In our previous study, we investigated the service lifetime of Ti_4O_7-NT-REM in a Na_2SO_4 solution and reported that the REM's service lifetime was 288.2 h [31]. To gain further insight into the service lifetime of Ti_4O_7-NT-REM in an actual ROC treatment, accelerated service life tests were performed with actual ROCs (Figure 6). As shown in Figure 6, the service lifetime of Ti_4O_7-NT-REM in the actual ROC was 267.3 h, which was slightly shorter than that in the Na_2SO_4 solution. This was not surprising because the ROC was much more complex than the Na_2SO_4 solution, and many ions in the ROC had a strong impact on the service lifetime, such as scaling by Ca^{2+} and Mg^{2+} or deactivation by the generated RCS. Moreover, considering that chloride ions were the most common anion in ROCs (Table S1), the REM's service lifetime was tested in a 0.5 M NaCl solution. The results show that the REM still has a relatively long service lifetime of 241.2 h, demonstrating strong resistance of Ti_4O_7-NT-REM to the chloride-induced corrosion.

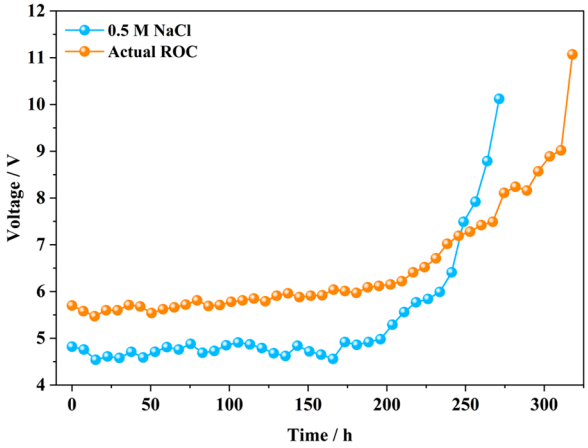

Figure 6. Accelerated service life test of Ti_4O_7-NT-REM in two solutions.

Besides the service lifetime, operating cost is also a crucial parameter of REMs in actual application [44]. Energy consumption (EC) is a common indicator used to evaluate operating costs. As shown in Table 1, the EC of Ti_4O_7-NT-REM was only 7.6 kWh·kg COD^{-1}, which was the lowest among all the listed electrodes or REMs. This is attributed mainly to the advantages of the flow-through mode together with the superior electrochemical characteristics of Ti_4O_7. In conclusion, the relatively long service life, excellent electrochemical stability (if continuous reverse polarity treatments are employed) as well as the low toxicity of titanium oxide indicated that Ti_4O_7-NT-REM technology is environmentally sustainable. Furthermore, the low EC together with the low fabrication cost of ~USD 0.36 per m^2 (including this study) indicated that this technology also is economically sustainable [29]. Thus, Ti_4O_7-NT-REM has exhibited promising potential for application in the treatment of ROC.

Table 1. A comparison of Ti_4O_7-NT-REM with other anodes in ROC treatment.

Anode	Operating Mode	Current Density	COD Removal	TOC Removal	Energy Consumption	Ref.
BDD	Flow-by	40 mA cm^{-2}	91.9%	76.63%	1500 kWh·kg COD^{-1}	[23]
Ti/TiO_2-NTs/PbO_2	Flow-by	40 mA cm^{-2}	47.59%	/	190 kWh·kg COD^{-1}	[45]
BDD	Batch	25 mA/cm^{-2}	100%	/	158 kWh·kg COD^{-1}	[46]
BDD	Batch	5 mA/cm^{-2}	100%	/	59 kWh·kg COD^{-1}	[47]
Ti/IrO_2–Ta_2O_5	Batch	25 mA/cm^{-2}	<50%	/	50 kWh·kg COD^{-1}	[46]
Si/BDD	Flow-by	12.5 mA cm^{-2}	100%	~70%	34 kWh·kg COD^{-1}	[48]
Ti_4O_7-NT-REM	Flow-through	20 mA cm^{-2}	74%	68%	7.6 kWh·kg COD^{-1}	This study

4. Conclusions

In this work, Ti_4O_7-NT-REM was applied to treat actual ROCs. The results indicated that the REM performed well in terms of COD, TOC, NH_4^+-N and NO_3^--N removal, and the appropriate conditions were a current density of 15 mA cm^{-2}, a flow rate of 8 mL s^{-1} and a pH value of 7. The significant changes in DOM before and after treatment suggested that the organics in ROC were efficiently removed by the Ti_4O_7-NT-REM. The REM also exhibited stable performance in that 70~81% of the COD, 64~78% of the TOC, 99.1~100% of the NH_4^+-N and 68~75% of the NO_3^--N were removed during the cyclic experiments (20 cycles). An accelerated service life test indicated that Ti_4O_7-NT-REM possesses a relatively long service lifetime during actual ROC treatment. Energy consumption was as low as 7.6 kWh·kg COD^{-1} after calculation, which was competitive with many other electrochemical technologies and acceptable for engineering applications. However, actual ROC treatment engineering is not yet mature enough at this time; the pilot or above scale must be investigated, and reactor or device design is also needed before implementation.

Supplementary Materials: The following supporting information can be downloaded at https://www.mdpi.com/article/10.3390/w16243579/s1: Text S1: GC–MS analyses; Text S2: Calculation equations for removal and energy consumption; Table S1: Water quality of the collected actual reverse osmosis concentrates; Table S2: Organic composition of influent detected by GC–MS; Table S3: Organic composition of effluent detected by GC–MS. Figure S1: GC–MS analysis and proportions of DOM (a) before and (b) after treatment; Figure S2: Mechanism diagram of the generation of reactive species (·OH and RCS) and atomic H* as well as their attack on the organics; Figure S3. SEM images of Ti_4O_7-NT-REM (a) before and (b) after 20 cycles.

Author Contributions: Conceptualization, Q.Q. and Y.Z.; methodology, P.X., Y.G. and M.Y.; validation, F.W. and Y.L.; data curation, T.D., D.X. and C.G.; writing—original draft preparation, Q.Q.; writing—review and editing, Q.Q. and Y.Z.; supervision, F.W. and Y.L.; project administration, F.W. and Y.L. All authors have read and agreed to the published version of the manuscript.

Funding: This research is a project funded by the Natural Science Foundation of Jiangsu Province (No. BK20220697), the Natural Science Foundation of China (No. 52400059) and the Funding for School-Level Research Projects of Yancheng Institute of Technology (No. xjr2022029).

Data Availability Statement: The original contributions presented in this study are included in the article/Supplementary Materials. Further inquiries can be directed to the corresponding authors.

Conflicts of Interest: The authors declare no conflicts of interest.

References

1. Dos Santo, S.; Adams, E.A.; Neville, G.; Wada, Y.; Sherbinin, A.D.; Mullin Bernhardt, E.; Adamo, S.B. Urban growth and water access in sub-Saharan Africa: Progress, challenges, and emerging research directions. *Sci. Total Environ.* **2017**, *607–608*, 497–508. [CrossRef] [PubMed]
2. Xu, C.; Peng, Z.; Zhang, H.; He, Z. Study of Comprehensive Utilization of Water Resources of Urban Water Distribution Network. *Water* **2021**, *13*, 2791. [CrossRef]
3. Mousavi, S.S.; Kargari, A. Water recovery from reverse osmosis concentrate by commercial nanofiltration membranes: A comparative study. *Desalination* **2022**, *528*, 115619. [CrossRef]
4. Pérez-González, A.; Urtiaga, A.M.; Ibáñez, R.; Ortiz, I. State of the art and review on the treatment technologies of water reverse osmosis concentrates. *Water Res.* **2012**, *46*, 267–283. [CrossRef]
5. Yin, X.; Li, W.; Zhu, H.; Yu, J.; Wei, K.; Gao, Z.; Zhang, Y.; Chen, H.; Gu, L.; Han, W. Electrochemical treatment of municipal reverse osmosis concentrates by a TiO2-BNTs/SnO2-Sb reactive electrochemical membrane. *Sep. Purif. Technol.* **2024**, *331*, 125726. [CrossRef]
6. Li, H.; Liu, H. Treatment and recovery methods for leachate concentrate from landfill and incineration: A state-of-the-art review. *J. Clean. Prod.* **2021**, *329*, 129720. [CrossRef]
7. Almeida, R.D.; Porto, R.F.; Quintaes, B.R.; Bila, D.M.; Lavagnolo, M.C.; Campos, J.C. A review on membrane concentrate management from landfill leachate treatment plants: The relevance of resource recovery to close the leachate treatment loop. *Waste Manag. Res.* **2023**, *41*, 264–284. [CrossRef]
8. Meng, L.; Mansouri, J.; Li, X.; Liang, J.; Huang, M.; Lv, Y.; Wang, Z.; Chen, V. Omni phobic membrane via bioinspired silicification for the treatment of RO concentrate by membrane distillation. *J. Membr. Sci.* **2022**, *647*, 120267. [CrossRef]
9. Long, W.; Koo, J.W.; Yuan, Z.; She, Q. Flow-through electrochemically assisted reverse-osmosis: A new process towards low-chemical desalination. *Water Res.* **2024**, *249*, 120982. [CrossRef]
10. Bai, F.; Liu, S.; Zhang, Y.; Ma, J. Effective and mechanistic insights into reverse osmosis concentrate of landfill leachate treatment using coagulation-catalytic ozonation-bioaugmentation-based AnMBR. *Chem. Eng. J.* **2023**, *463*, 142430. [CrossRef]
11. Mangalgiri, K.; Cheng, Z.; Cervantes, S.; Spencer, S.; Liu, H. UV-based advanced oxidation of dissolved organic matter in reverse osmosis concentrate from a potable water reuse facility: A parallel-factor (PARAFAC) analysis approach. *Water Res.* **2021**, *204*, 117585. [CrossRef] [PubMed]
12. Ren, L.; Li, Y.; Guo, Y.; Yang, K.; Yi, Q.; Wang, X.; Wu, Z.; Wang, Z. Electrochemical oxidation of reverse osmosis concentrate using a pilot-scale reactive electrochemical membrane filtration system: Performance and mechanisms. *J. Hazard. Mater.* **2024**, *465*, 133315. [CrossRef] [PubMed]
13. Gong, C.; Ren, X.; Han, J.; Wu, Y.; Gou, Y.; Zhang, Z.; He, P. Toxicity reduction of reverse osmosis concentrates from petrochemical wastewater by electrocoagulation and fered-Fenton treatments. *Chemosphere* **2022**, *286*, 131582. [CrossRef] [PubMed]
14. Cui, T.; Wang, X.; Chen, Y.; Fu, B.; Tu, Y. Reverse Osmosis Coupling Multi-Catalityc Ozonation (RO-MCO) in Treating Printing and Dyeing Wastewater and Membrane concentrate: Removal performance and Mechanism. *Water Resour. Ind.* **2023**, *30*, 100217. [CrossRef]
15. Bagastyo, A.Y.; Radjenovic, J.; Mu, Y.; Rozendal, R.A.; Batstone, D.J.; Rabaey, K. Electrochemical oxidation of reverse osmosis concentrate on mixed metal oxide (MMO) titanium coated electrodes. *Water Res.* **2011**, *45*, 4951–4959. [CrossRef]

16. Hui, H.; Wang, H.; Mo, Y.; Yin, Z.; Li, J. Optimal design and evaluation of electrocatalytic reactors with nano-MnOx/Ti membrane electrode for wastewater treatment. *Chem. Eng. J.* **2019**, *376*, 120190. [CrossRef]
17. Hui, H.; Wang, H.; Mo, Y.; Li, L.; Yin, Z.; He, B.; Li, J.; Wang, T. A three-stage fixed-bed electrochemical reactor for biologically treated landfill leachate treatment. *Chem. Eng. J.* **2019**, *376*, 121026. [CrossRef]
18. Lin, H.; Peng, H.X.; Feng Li, X.; Zhao, J.; Yang, K.; Yang, K.; Liao, J.; Cheng, D.; Liu, X.; Lv, S.; et al. Energy-efficient for advanced oxidation of bio-treated landfill leachate effluent by reactive electrochemical membranes (REMs): Laboratory and pilot scale studies. *Water Res.* **2021**, *190*, 116790. [CrossRef]
19. Guvenc, S.; Bayat, M.; Can-Güven, E.; Varank, G. Hybrid and combined electro-oxidation and peroxi-coagulation processes in effective treatment of textile reverse osmosis concentrate. *Chem. Eng. Sci.* **2024**, *298*, 120365. [CrossRef]
20. He, L.; Ji, Y.; Cheng, J.; Wang, C.; Jiang, L.; Chen, X.; Li, H.; Ke, S.; Wang, J. Effect of pH and Cl^- concentration on the electrochemical oxidation of pyridine in low-salinity reverse osmosis concentrate: Kinetics, mechanism, and toxicity assessment. *Chem. Eng. J.* **2022**, *449*, 137669. [CrossRef]
21. Zhao, C.; Wu, Z.; Lai, J.; Liu, L.; Li, H.; Wang, H. Efficient electrochemical oxidation of refractory organics in actual petrochemical reverse osmosis concentrates by Ti/SnO_2-Sb mesh anode. *Process Saf. Environ.* **2024**, *182*, 1060–1071. [CrossRef]
22. Liao, D.; Chen, Y.; Yin, F.; Lv, B.; Wu, F.; Xie, J.; Feng, D. Performance of electrochemical treatment of refractory organic matter in printing and dyeing reverse osmosis concentrate. *J. Environ. Chem. Eng.* **2023**, *11*, 109173. [CrossRef]
23. Weng, M.; Pei, J. Electrochemical oxidation of reverse osmosis concentrate using a novel electrode: Parameter optimization and kinetics study. *Desalination* **2016**, *399*, 21–28. [CrossRef]
24. Liu, N.; Zhao, X.; Wang, C.; Li, Y.; Pan, S.; Huang, W.; Hakizimana, I.; Kong, W.; Wang, Y. Application of electrochemical flow-through oxidation technology in the treatment of concentrated water from nanofiltration and reverse osmosis in the coal chemical industry. *J. Environ. Chem. Eng.* **2024**, *12*, 114663. [CrossRef]
25. Comninellis, C. Electrocatalysis in the electrochemical conversion/combustion of organic pollutants for waste-water treatment. *Electrochim. Acta* **1994**, *39*, 1857–1862. [CrossRef]
26. Chaplin, B.P. Critical review of electrochemical advanced oxidation processes for water treatment applications. *Environ. Sci. Process. Impacts* **2014**, *16*, 1182–1203. [CrossRef]
27. Li, X.; Pletcher, D.; Walsh, F.C. Electrodeposited lead dioxide coatings. *Chem. Soc. Rev.* **2011**, *40*, 3879–3894. [CrossRef]
28. Chaplin, B.P. The prospect of electrochemical technologies advancing worldwide water treatment. *Accounts Chem. Res.* **2019**, *52*, 596–604. [CrossRef]
29. Bejan, D.; Malcolm, J.; Morrison, L.; Bunce, N. Mechanistic investigation of the conductive ceramic Ebonex® as an anode material. *Electrochim. Acta* **2009**, *54*, 5548–5556. [CrossRef]
30. Zhao, L.; Fan, W.; Chen, T.X.; Tang, J.Z.; Liu, Y.; Jia, H.Z.; Li, J.; Yao, J.L.; Liu, B.D. A novel synthetic strategy of mesoporous Ti_4O_7-coated electrode for highly efficient wastewater treatment. *Ceram. Int.* **2024**, *50*, 26503–26512. [CrossRef]
31. Zhang, Y.; Song, Y.; Liu, L.; Zhang, J.; Zhang, Z.; Li, Q.; Yang, J.; Li, W.; Huang, L.; Li, X.; et al. Electrochemical treatment of antibiotic wastewater containing ceftriaxone sodium by porous Ti/Magnéli Ti_4O_7 nanotube arrays. *Water Resour. Ind.* **2024**, *31*, 100235. [CrossRef]
32. Geng, P.; Su, J.Y.; Miles, C.; Comninellis, C.; Chen, G.H. Highly-ordered Magneli Ti_4O_7 nanotube arrays as effective anodic material for electro-oxidation. *Electrochim. Acta* **2015**, *153*, 316–324. [CrossRef]
33. Zhou, S.; Watanabe, H.; Wei, C.; Wang, D.; Zhou, J.; Tatarazako, N.; Masunaga, S.; Zhang, Y. Reduction in toxicity of coking wastewater to aquatic organisms by vertical tubular biological reactor. *Ecotoxicol. Environ. Saf.* **2015**, *115*, 217–222. [CrossRef] [PubMed]
34. Zhang, Y.; Gu, L.; Zhang, Y.; Yang, J.; Li, Q.; Yu, S.; Li, C.; Wei, K. Energy-efficient reuse of bio-treated textile wastewater by a porous-structure electrochemical PbO_2 filter: Performance and mechanism. *Environ. Res.* **2023**, *231*, 116254. [CrossRef]
35. Zhang, Y.H.; Wei, K.J.; Xu, A.L.; Han, W.Q.; Sun, X.Y.; Li, J.S.; Shen, J.Y.; Wang, L.J. Pesticide tailwater deeply treated by tubular porous electrode reactor (TPER): Purpose for discharging and cost saving. *Chemosphere* **2017**, *185*, 86–93. [CrossRef]
36. Guo, D.; Liu, Y.; Ji, H.; Wang, C.; Chen, B.; Shen, C.; Li, F.; Wang, Y.; Lu, P.; Liu, W. Silicate-enhanced heterogeneous flow-through electro-fenton system using iron oxides under nanoconfinement. *Environ. Sci. Technol.* **2021**, *55*, 4045–4053. [CrossRef]
37. Samet, Y.; Elaoud, S.C.; Ammar, S.; Abdelhedi, R. Electrochemical degradation of 4-chloroguaiacol for wastewater treatment using PbO_2 anodes. *J. Hazard. Mater.* **2006**, *138*, 614–619. [CrossRef]
38. Zheng, W.; Zhu, L.; Liang, S.; Ye, J.; Yang, X.; Lei, Z.; Yan, Z.; Li, Y.; Wei, C.; Feng, C. Discovering the Importance of ClO• in a coupled electrochemical system for the simultaneous removal of carbon and nitrogen from secondary coking wastewater effluent. *Environ. Sci. Technol.* **2020**, *54*, 9015–9024. [CrossRef]
39. Zheng, W.; Zhu, L.; Yan, Z.; Lin, Z.; Lei, Z.; Zhang, Y.; Xu, H.; Dang, Z.; Wei, C.; Feng, C. Self-activated Ni cathode for electrocatalytic nitrate reduction to ammonia: From fundamentals to scale-up for treatment of industrial wastewater. *Environ. Sci. Technol.* **2021**, *55*, 13231–13243. [CrossRef]
40. Chen, M.; Pan, S.; Zhang, C.; Wang, C.; Zhang, W.; Chen, Z.; Zhao, X.; Zhao, Y. Electrochemical oxidation of reverse osmosis concentrates using enhanced TiO_2-NTA/SnO_2-Sb anodes with/without PbO_2 layer. *Chem. Eng. J.* **2020**, *399*, 125756. [CrossRef]
41. Chang, H.; Hu, R.; Zou, Y.; Quan, X.; Zhong, N.; Zhao, S.; Sun, Y. Highly efficient reverse osmosis concentrate remediation by microalgae for biolipid production assisted with electrooxidation. *Water Res.* **2020**, *174*, 115642. [CrossRef] [PubMed]

42. Zhang, Y.; Tang, W.; Bai, J.; Li, J.; Wang, J.; Zhou, T.; Guan, X.; Zhou, B. Highly efficient removal of total nitrogen and dissolved organic compound in waste reverse osmosis concentrate mediated by chlorine radical on 3D Co_3O_4 nanowires anode. *J. Hazard. Mater.* **2022**, *424*, 127662. [CrossRef] [PubMed]
43. *GB16889-2008*; Standard for Pollution Control on the Landfill Site of Municipal Solid Waste. China Environmental Publishing Group: Beijing, China, 2008.
44. Ansari, A.; Nematollahi, D. Convergent paired electrocatalytic degradation of p-dinitrobenzene by Ti/SnO_2-Sb/β-PbO_2 anode. A new insight into the electrochemical degradation mechanism. *Water. Res.* **2018**, *144*, 462–473. [CrossRef]
45. Wei, F.; Liao, D.; Lin, Y.; Hu, C.; Ju, J.; Chen, Y.; Feng, D. Electrochemical degradation of reverse osmosis concentrate (ROC) using the electrodeposited Ti/TiO_2-NTs/PbO_2 electrode. *Sep. Purif. Technol.* **2021**, *258*, 118056. [CrossRef]
46. Zhou, M.; Liu, L.; Jiao, Y.; Wang, Q.; Tan, Q. Treatment of high-salinity reverse osmosis concentrate by electrochemical oxidation on BDD and DSA electrodes. *Desalination* **2011**, *277*, 201–206. [CrossRef]
47. P′erez, G.; Fern′andez-Alba, A.R.; Urtiaga, A.M.; Ortiz, I. Electro-oxidation of reverse osmosis concentrates generated in tertiary water treatment. *Water Res.* **2010**, *44*, 2763–2772. [CrossRef]
48. Bagastyo, A.Y.; Batstone, D.J.; Kristiana, I.; Escher, B.I.; Joll, C.; Radjenovic, J. Electrochemical treatment of reverse osmosis concentrate on boron-doped electrodes in undivided and divided cell configurations. *J. Hazard. Mater.* **2014**, *279*, 111–116. [CrossRef]